Satellite Attitude Control and Power Tracking with Energy/Momentum Wheels

Panagiotis Tsiotras* and Haijun Shen†
Georgia Institute of Technology
Atlanta, GA 30332-0150, USA

Chris Hall‡
Virginia Polytechnic Institute and State University
Blacksburg, VA 24061-0203, USA

A control law for an Integrated Power/Attitude Control System (IPACS) for a satellite is presented in this paper. Four or more energy/momentum wheels in an arbitrary non-coplanar configuration and a set of three thrusters are used to implement the torque inputs. The energy/momentum wheels are used as attitude control actuators, as well as an energy storage mechanism, providing power to the spacecraft. In that respect, they can replace the currently used heavy chemical batteries. The thrusters are used to implement the torques for large and fast (slew) maneuvers during the attitude initialization and target acquisition phases and to implement the momentum management strategies. The energy/momentum wheels are used to provide the reference-tracking torques and the torques for spinning up or down the wheels for storing and releasing kinetic energy. The controller published in a previous work by the authors is adopted here for the attitude tracking function of the wheels. Power tracking for charging and discharging the wheels is added to complete the IPACS framework. The torques applied by the energy/momentum wheels are decomposed into two spaces which are orthogonal to each other, with the attitude control torques and power tracking torques in each space. This control law can be easily incorporated in an IPACS system on-board a satellite. The possibility of occurrence of singularities, where no arbitrary energy profile can be tracked, is studied for a generic wheel cluster configuration. A standard momentum management scheme is considered to null the total angular momentum of the wheels so as to minimize the gyroscopic effects and prevent the singularity from occurring. A numerical example for a satellite in a low Earth near-polar orbit is provided to test the proposed IPACS algorithm. The satellite's boresight axis is required to track a ground station, while the satellite is required to rotate about its boresight axis so that the solar panel axis is perpendicular to the satellite-Sun vector.

Introduction

Most spacecraft use chemical batteries (usually, NiCd, NiH_2) to store excess energy generated by the solar panels during periods of exposure to the Sun.[1] During eclipse, the batteries are used to provide power for the spacecraft subsystems. The batteries are recharged when the spacecraft is in the sunlight. The primary problem with this approach is the cycle life of batteries and the additional power system mass required to control the charging and discharging cycles. Chemical batteries have shallow discharge depth (about 20% to 30% of their rated energy storage capacity), large weight, and require operation within strict temperature limits (at or below 20°C in a low earth orbit) which often drive the entire spacecraft thermal design.

An alternative to chemical batteries is the use of flywheels to store energy. The use of flywheels has the benefit of increased efficiency (up to 90% depth of discharge with essentially unlimited life), operation in a relatively hot (up to 40°C) environment, and the potential to combine the energy storage and attitude control functions into a single device, thus increasing reliability, and reducing overall weight and spacecraft size. This concept, termed the Integrated Power and Attitude Control System (IPACS) has been studied since the 1960s, but it has been particularly popular since the 1980s. In fact, the use of flywheels instead of batteries to store energy on spacecraft was suggested as early as 1961 in the article by Roes,[2] when a 17 Whr/kg composite flywheel spinning at 10,000 to 20,000 rpm on magnetic bearings was proposed. The configuration included two counter-rotating flywheels, and the author did not mention the possibility of using the momentum for attitude control. However, since many spacecraft use flywheels (in the form of momentum wheels, control moment gyros, etc.) to control attitude, the integration of these two functions is naturally of great interest. Numerous studies of this integration have been conducted. Anderson and Keckler[3] originated the term "IPACS" in 1973. A study by Cormack[4] done for Rockwell examined the use of an integrated IPACS system. Keckler and Jacobs[5] presented a description of the concept. Will *et al.*[6] investigated the IPACS concept and performed simulations using the (lin-

*Associate Professor, School of Aerospace Engineering, Georgia Institute of Technology. Email: p.tsiotras@ae.gatech.edu. Senior member AIAA.

†Graduate Student, School of Aerospace Engineering, Georgia Institute of Technology. Email: gt7318d@prism.gatech.edu. Student member AIAA.

‡Associate Professor, Department of Aerospace and Ocean Engineering, Virginia Polytechnic Institute and State University, Email: chall@aoe.vt.edu. Associate Fellow AIAA.

earized) equations of motion. Notti *et al.*[7] performed an extensive systems study and investigated linear control laws for attitude control. Their study included trade studies on the use of momentum wheels, control moment gyros, and counter-rotating pairs. NASA and Boeing also conducted separate studies on the IPACS concept.[8,9] Anand *et al.*[10,11] discussed the system design issues associated with using magnetic bearings, as did Downer *et al.*[12] Flatley[13] studied a tetrahedron array of four momentum wheels, and considered the issues associated with simultaneously torquing the wheels for attitude control and energy storage. Around the same time with Flatley's work, O'Dea *et al.*[14] included simultaneous attitude determination in their study of a combined Attitude, Reference, and Energy Storage (CARES) system, focusing on technology-related issues. Oglevie and Eisenhaure[15,16] performed a system level study of IPACS systems. Reference 15 includes a substantial list of references to earlier work. Olmsted[17] presented technology-related issues associated with a particular flywheel design. Optimal design criteria associated with an integrated Attitude Control and Energy Storage (ACES) system have been discussed by Studer and Rodriguez.[18]

Most of these previous investigations of IPACS focus on general design issues. The exact nonlinear equations of motions are not considered even when the attitude control results are provided. In this paper, the exact nonlinear equations of motion are used to design an attitude controller which tracks a reference attitude profile. The wheel control torque space is decomposed into two spaces which are orthogonal to each other. The attitude control torques lie in one of these two spaces, and the torques in the other space are used to spin up or down the energy/momentum wheels to store or extract kinetic energy. In the following, the system model is given first, then the reference attitude and energy/momentum wheel power tracking controllers are presented. A numerical example considering a Iridium-type satellite[19] in orbit is provided to illustrate the proposed IPACS methodology.

It should be pointed out that flywheels used in an IPACS system typically rotate at much higher speeds than standard momentum wheels, since their operation is driven primarily by the energy storage function than the attitude control function. In this paper, we use the term "energy/momentum" wheels to emphasize this difference with commonly used momentum wheels.

System model

Dynamics

Consider a rigid spacecraft with an N-wheel cluster installed to provide internal torques. Let **B** denote the spacecraft body frame. Then the rotational equations of motion for the spacecraft can be expressed as

$$\dot{\mathbf{h}}_B = \mathbf{h}_B^{\times}\mathbf{J}^{-1}(\mathbf{h}_B - \mathbf{A}\mathbf{h}_a) + \mathbf{g}_e \tag{1a}$$

$$\dot{\mathbf{h}}_a = \mathbf{g}_a \tag{1b}$$

where $\mathbf{h}_B$ is the angular momentum vector of the spacecraft in the **B** frame, given by

$$\mathbf{h}_B = \mathbf{J}\boldsymbol{\omega}_B + \mathbf{A}\mathbf{h}_a \tag{2}$$

where $\mathbf{h}_a$ is the $N \times 1$ vector of the *axial* angular momenta of the wheels, $\boldsymbol{\omega}_B$ is the angular velocity vector of the spacecraft in the **B** frame, $\mathbf{g}_e$ is the 3×1 vector of external torques, $\mathbf{g}_a$ is the $N \times 1$ vector of the internal axial torques applied by the platform to the wheels, and $\mathbf{A}$ is the $3 \times N$ matrix whose columns contain the axial unit vectors of the N energy/momentum wheels. $\mathbf{J}$ is an inertia-like matrix defined as

$$\mathbf{J} = \mathbf{I} - \mathbf{A}\mathbf{I}_s\mathbf{A}^T \tag{3}$$

where $\mathbf{I}$ is the moment of inertia of the spacecraft, including the wheels and $\mathbf{I}_s = \mathrm{diag}\{\mathbf{I}_{s1}, \mathbf{I}_{s2}, \ldots, \mathbf{I}_{sN}\}$ is a diagonal matrix with the axial moments of inertia of the wheels.

The *axial* angular momentum vector of the wheels can be written as

$$\mathbf{h}_a = \mathbf{I}_s\mathbf{A}^T\boldsymbol{\omega}_B + \mathbf{I}_s\boldsymbol{\omega}_s \tag{4}$$

where $\boldsymbol{\omega}_s = (\omega_{s1}, \omega_{s2}, \ldots, \omega_{sN})^T$ is an $N \times 1$ vector denoting the axial angular velocity of the energy/momentum wheels with respect to the spacecraft. We denote the total axial angular velocity of the wheels relative to the inertial frame as $\boldsymbol{\omega}_c = (\omega_{c1}, \omega_{c2}, \ldots, \omega_{cN})^T$. Using this notation, Eq. (4) can be written as

$$\mathbf{h}_a = \mathbf{I}_s\boldsymbol{\omega}_c \tag{5}$$

where, $\boldsymbol{\omega}_c = \boldsymbol{\omega}_s + \mathbf{A}^T\boldsymbol{\omega}_B$. Notice that since typically the wheels spin at a much higher speed than the spacecraft itself, $\boldsymbol{\omega}_s >> \boldsymbol{\omega}_B$ and we have that $\boldsymbol{\omega}_c \approx \boldsymbol{\omega}_s$.

In Eq. (1) the external torques are assumed to include the control torque due to thruster firing, the gravity gradient torque and the other disturbance torques; i.e.,

$$\mathbf{g}_e = \mathbf{g}_t + \mathbf{g}_g + \mathbf{g}_d \tag{6}$$

where the subscripts t, g, and d denote the thruster, gravity gradient, and disturbance, respectively. The gravity gradient torque is given by[20]

$$\mathbf{g}_g = \frac{3\mu}{R_c^3}\hat{\mathbf{c}}_3^{\times}\mathbf{I}\hat{\mathbf{c}}_3 \tag{7}$$

where $\hat{\mathbf{c}}_3$ is the unit vector $-\mathbf{r}_c/R_c$ (the same as $\hat{\mathbf{z}}_l$, the z-axis of the Local Vertical Local Horizontal (LVLH) frame, shown in Fig. 3) expressed in the body frame, with $\mathbf{r}_c$ the vector from the earth center to the spacecraft center of mass with $R_c = |\mathbf{r}_c|$, and $\mu = 3.986005 \times 10^5 \mathrm{km}^3\mathrm{s}^{-2}$ is

the constant gravitational parameter. It should be pointed out that although we restrict the discussion to external control torques due to thruster firing, our approach remains the same for other choices of actuators, such as magnetotorquers, etc.

Kinematics

The so-called "Modified Rodrigues Parameters" (MRPs) given in Refs. 21, 22 will be chosen to describe the attitude kinematics *error* of the spacecraft. The MRPs are defined in terms of the Euler principal unit vector, $\hat{\mathbf{e}}$, and angle ϕ, by

$$\boldsymbol{\sigma} = \hat{\mathbf{e}} \tan(\phi/4) \tag{8}$$

The MRPs have the advantage of being well-defined for the whole range for rotations, i.e., $\phi \in [0, 2\pi)$. The differential equation governing the kinematics in terms of the MRPs is given by[21]

$$\dot{\boldsymbol{\sigma}} = \mathbf{G}(\boldsymbol{\sigma})\boldsymbol{\omega} \tag{9}$$

where

$$\mathbf{G}(\boldsymbol{\sigma}) = \frac{1}{2}\left(\mathbf{1} + \boldsymbol{\sigma}^{\times} + \boldsymbol{\sigma}\boldsymbol{\sigma}^{T} - \frac{1+\boldsymbol{\sigma}^{T}\boldsymbol{\sigma}}{2}\mathbf{1}\right) \tag{10}$$

and $\mathbf{1}$ is the 3×3 identity matrix.

Tracking controller

In the previous work by the authors,[23] three control laws were presented to track a reference attitude profile using coordinated action of both thrusters and momentum wheels. Here we restate the controller II from Ref. 23 which will be used for attitude tracking. This control law assumes that the reference frame dynamics and kinematics are given by

$$\dot{\mathbf{h}}_R = \mathbf{h}_R^{\times}\mathbf{J}^{-1}\mathbf{h}_R + \mathbf{g}_R \tag{11}$$

$$\dot{\boldsymbol{\sigma}}_R = \mathbf{G}(\boldsymbol{\sigma}_R)\boldsymbol{\omega}_R \tag{12}$$

where the subscript R stands for the reference frame to be tracked (referred to later as the "desired" or "target" frame) and where $\mathbf{h}_R = \mathbf{J}\boldsymbol{\omega}_R$.

Given the reference attitude history to be tracked from Eqs. (11) and (12), the angular velocity tracking error in the body frame is

$$\delta\boldsymbol{\omega} = \boldsymbol{\omega}_B - \mathbf{C}_R^B(\delta\boldsymbol{\sigma})\boldsymbol{\omega}_R \tag{13}$$

where $\mathbf{C}_R^B(\delta\boldsymbol{\sigma})$ is the rotation matrix from the reference frame $\mathbf{R}$ to the body frame $\mathbf{B}$, and $\delta\boldsymbol{\sigma}$ is the MRP vector between the reference frame and the body frame; i.e.,

$$\mathbf{C}_R^B(\delta\boldsymbol{\sigma}) = \mathbf{C}_N^B[\mathbf{C}_N^R]^T \tag{14}$$

and the attitude error satisfies the following differential equation

$$\delta\dot{\boldsymbol{\sigma}} = \mathbf{G}(\delta\boldsymbol{\sigma})\delta\boldsymbol{\omega} \tag{15}$$

A feedback control law to render $\delta\boldsymbol{\omega} \to 0$ and $\delta\boldsymbol{\sigma} \to 0$ is found by using the following Lyapunov function

$$V = \frac{1}{2}\delta\boldsymbol{\omega}^T\mathbf{J}^{-1}\delta\boldsymbol{\omega} + 2k_2\ln(1+\delta\boldsymbol{\sigma}^T\delta\boldsymbol{\sigma}) \tag{16}$$

where $k_2 > 0$. This function is positive definite and radially unbounded[21] in terms of the tracking errors $\delta\boldsymbol{\omega}$ and $\delta\boldsymbol{\sigma}$. Taking the derivative of V and using Eqs. (13) and (15) yields the time derivative of V in terms of $\boldsymbol{\omega}_B$, $\boldsymbol{\omega}_R$ and the tracking error $\delta\boldsymbol{\omega}$ and $\delta\boldsymbol{\sigma}$, i.e.,

$$\begin{aligned}\dot{V} =& \delta\boldsymbol{\omega}^T\left[\mathbf{h}_B^{\times}\mathbf{J}^{-1}(\mathbf{h}_B - \mathbf{A}\mathbf{h}_a) + \mathbf{g}_t + \mathbf{g}_g - \mathbf{J}\boldsymbol{\omega}_B^{\times}\delta\boldsymbol{\omega}\right.\\ &-\mathbf{J}\mathbf{C}_R^B(\delta\boldsymbol{\sigma})\mathbf{J}^{-1}\mathbf{h}_R^{\times}\mathbf{J}^{-1}\mathbf{h}_R - \mathbf{J}\mathbf{C}_R^B(\delta\boldsymbol{\sigma})\mathbf{J}^{-1}\mathbf{g}_R\\ &\left.-\mathbf{A}\mathbf{g}_a + k_2\delta\boldsymbol{\sigma}\right]\end{aligned} \tag{17}$$

The external torque, $\mathbf{g}_t$, is typically chosen to effect a desired large-angle attitude correction, whereas the internal torques, $\mathbf{g}_a$, are chosen to eliminate errors. For any external torque, if we select the internal torques such that

$$\begin{aligned}\mathbf{A}\mathbf{g}_a =& \mathbf{h}_B^{\times}\mathbf{J}^{-1}(\mathbf{h}_B - \mathbf{A}\mathbf{h}_a) + \mathbf{g}_t + \mathbf{g}_g - \mathbf{J}\boldsymbol{\omega}_B^{\times}\delta\boldsymbol{\omega}\\ &- \mathbf{J}\mathbf{C}_R^B(\delta\boldsymbol{\sigma})\mathbf{J}^{-1}\mathbf{h}_R^{\times}\mathbf{J}^{-1}\mathbf{h}_R - \mathbf{J}\mathbf{C}_R^B(\delta\boldsymbol{\sigma})\mathbf{J}^{-1}\mathbf{g}_R\\ &+ k_1\delta\boldsymbol{\omega} + k_2\delta\boldsymbol{\sigma}\end{aligned} \tag{18}$$

with $k_1 > 0$, the derivative of the Lyapunov function is

$$\dot{V} = -k_1\delta\boldsymbol{\omega}^T\delta\boldsymbol{\omega} \leq 0 \tag{19}$$

As shown in Ref. 23, the tracking error system is asymptotically stable; i.e., $\boldsymbol{\omega}_B \to \boldsymbol{\omega}_R$, and $\boldsymbol{\sigma}_B \to \boldsymbol{\sigma}_R$ as $t \to \infty$.

Equation (18) allows for a variety of different control actions. In particular, once the thruster control action $\mathbf{g}_t$ has been chosen, the energy/momentum wheel action is computed directly from (18). Later on, we will use this equation to design control laws during two different phases of the satellite operation, namely the target acquisition (attitude initialization) phase and the attitude/power tracking phase. We also point out that in the absence of initial errors ($\delta\boldsymbol{\omega}(0) = \delta\boldsymbol{\sigma}(0) = 0$) and for initial wheel axial momentum zero, $\mathbf{h}_a(0) = 0$, Eq. (18) reduces to $\mathbf{A}\mathbf{g}_a = 0$ and $\mathbf{g}_t = \mathbf{g}_R - \mathbf{g}_g$.

Given the torque action $\mathbf{g}_t$, we denote the right hand side of Eq. (18) by $\mathbf{f}$. The internal torque provided by the wheels, $\mathbf{g}_a$, is given by solving the linear system $\mathbf{A}\mathbf{g}_a = \mathbf{f}$. If $N < 3$, this system is overdetermined and a solution may not exist; if $N = 3$, (and for non-coplanar wheels), the solution is uniquely determined; and if $N > 3$, the system is underdetermined and there exists an infinite number of solutions. In particular, in the latter case every solution has the form $\mathbf{g}_a = \mathbf{g}_r + \mathbf{g}_n$, where $\mathbf{g}_r$ belongs to the range space $R(\mathbf{A}^T)$ of the matrix $\mathbf{A}^T$ and $\mathbf{g}_n$ belongs to the null space $N(\mathbf{A})$ of the matrix $\mathbf{A}$.

It is seen that $\mathbf{g}_n$ does not contribute to the attitude control input since $\mathbf{A}\mathbf{g}_n = 0$. One can always choose the torque $\mathbf{g}_r$ to fulfill the equation $\mathbf{A}\mathbf{g}_r = \mathbf{f}$, and subsequently use $\mathbf{g}_n$ to perform power/energy storage management.[24] Notice that this approach can be implemented as long as $N(\mathbf{A})$ has nonzero dimension, which is always true for a cluster with more than three non-coplanar wheels.

In the following section, we will consider a general momentum-wheel cluster and construct the torques in the null space of $\mathbf{A}$, so as not to disturb the attitude control operation of the spacecraft, and to track a desired power profile. In other words, the power and attitude tracking operations are performed simultaneously and independent of one another. Power tracking objectives do not interfere with attitude tracking objectives and vice versa. We insist on this separation of objectives since it is unlikely that any IPACS system which compromises either power or attitude control requirement will be acceptable for use in routine spacecraft operations.

Power tracking

As shown in the previous section, the energy/momentum wheel torque required to control the attitude is given by an expression of the form

$$\mathbf{A}\mathbf{g}_a = \mathbf{f} \tag{20}$$

where $\mathbf{f}$ is the 3×1 required torque vector. The general solution for $\mathbf{g}_a$ is given by

$$\mathbf{g}_a = \mathbf{A}^+\mathbf{f} + \mathbf{g}_n \tag{21}$$

where $\mathbf{A}^+ = \mathbf{A}^T(\mathbf{A}\mathbf{A}^T)^{-1}$ is the projection operator on the range of $\mathbf{A}^T$, and thus $\mathbf{A}^+\mathbf{f} = \mathbf{g}_r \in R(\mathbf{A}^T)$, and where $\mathbf{g}_n \in N(\mathbf{A})$; i.e.,

$$\mathbf{A}\mathbf{g}_n = 0 \tag{22}$$

Note that $\mathbf{A}\mathbf{g}_a = \mathbf{A}(\mathbf{A}^+\mathbf{f} + \mathbf{g}_n) = \mathbf{f}$, so $\mathbf{g}_n$ does not affect the spacecraft motion.

The total kinetic energy stored in the wheels is

$$T = \frac{1}{2}\boldsymbol{\omega}_c^T \mathbf{I}_s \boldsymbol{\omega}_c \tag{23}$$

The power (rate of change of the energy), is given by

$$\frac{\mathrm{d}T}{\mathrm{d}t} = P = \boldsymbol{\omega}_c^T \mathbf{I}_s \dot{\boldsymbol{\omega}}_c \tag{24}$$

The objective here is to find a controller $\mathbf{g}_n$ in the null space of $\mathbf{A}$ to provide the required power function $P(t)$. Equation (5) implies that $\mathbf{g}_a = \dot{\mathbf{h}}_a = \mathbf{I}_s \dot{\boldsymbol{\omega}}_c$, so from Eq. (24) we have

$$\boldsymbol{\omega}_c^T \mathbf{g}_a = P \tag{25}$$

Therefore, simultaneous attitude control and power management requires a control torque vector $\mathbf{g}_a$ satisfying the following set of linear equations

$$\begin{bmatrix} \mathbf{A} \\ \boldsymbol{\omega}_c^T \end{bmatrix} \mathbf{g}_a = \begin{bmatrix} \mathbf{f} \\ P \end{bmatrix} \tag{26}$$

From Eq. (21), we have that the torque $\mathbf{g}_n$ in the null space of $\mathbf{A}$ has to satisfy

$$\boldsymbol{\omega}_c^T(\mathbf{A}^+\mathbf{f} + \mathbf{g}_n) = P \tag{27}$$

or letting the "modified power" $P_m = P - \boldsymbol{\omega}_c^T \mathbf{A}^+\mathbf{f}$,

$$\boldsymbol{\omega}_c^T \mathbf{g}_n = P_m \tag{28}$$

Since $\mathbf{g}_n \in N(A)$, there always exists a vector $\nu \in \mathbb{R}^N$ such that

$$\mathbf{g}_n = P_N \nu \tag{29}$$

where $P_N = \mathbf{1}_N - \mathbf{A}^T(\mathbf{A}\mathbf{A}^T)^{-1}\mathbf{A}$ is the (orthogonal) projection on $N(A)$. Thus, we have $\boldsymbol{\omega}_c^T P_N \nu = P_m$, to which a minimum norm solution is given by

$$\nu = P_N \boldsymbol{\omega}_c (\boldsymbol{\omega}_c^T P_N \boldsymbol{\omega}_c)^{-1} P_m \tag{30}$$

and the energy management torque $\mathbf{g}_n$ can then be chosen as

$$\mathbf{g}_n = P_N \boldsymbol{\omega}_c (\boldsymbol{\omega}_c^T P_N \boldsymbol{\omega}_c)^{-1} P_m \tag{31}$$

A solution of Eq. (31) exists, as long as $P_N \boldsymbol{\omega}_c \neq 0$. This implies, that either $\boldsymbol{\omega}_c \neq 0$ or $\boldsymbol{\omega}_c \notin N(\mathbf{A})^\perp = R(\mathbf{A}^T)$. The last requirement is also evident from Eq. (26), where the matrix in the left hand side does not have full row rank if $\boldsymbol{\omega}_c \in R(\mathbf{A}^T)$.

It should be pointed out that for satellite applications, during sunlight the solar panels provide enough power for the spacecraft equipment, and the wheels spin up to absorb and store the excess energy. Since the sunlight period is longer than the eclipse period, tracking a specific power function is less significant during the sunlight than during the eclipse period when the power is solely provided by spinning down the wheels. Some authors have therefore chosen to discard power tracking altogether and simply spin up the wheels during sunlight to store the excess energy. This is the approach used, for example, in Ref. 13. On the contrary, unloading of the wheels during the eclipse is more critical, since the wheel deceleration should be done at a certain *rate* in order to provide the necessary power to the spacecraft bus.

Singularity Avoidance and Momentum Management

So far, we have found a controller $\mathbf{g}_a$ which tracks desired power profiles, while controlling the spacecraft attitude. In addition, as was mentioned already, from Eq. (28) we can see that if $\boldsymbol{\omega}_c$ lies in the range space of $\mathbf{A}^T$, then since $\mathbf{g}_n$ is in the null space of $\mathbf{A}$, we have

$$\boldsymbol{\omega}_c^T \mathbf{g}_n = 0 \tag{32}$$

This case will be termed as singular, which implies that the controller loses the capability of tracking an arbitrary power function, and from Eq. (27) the only power the wheels can supply is $\boldsymbol{\omega}_c^T \mathbf{A}^+ \mathbf{f}$. However, the latter case is undesirable in many practical applications. For example, for a stabilized spacecraft when the torque $\mathbf{f}$ is small, the amount of supplied power can be less than the required power level during the singularity.

For a three-axis stabilized satellite, if the angular momenta of the wheels are not distributed such that the total angular momentum of the wheels stays close to zero, the gyroscopic effects will play a significant role, increasing the required torque for the attitude control. Hence in the following, a momentum management scheme will be included such that the total angular momentum of the wheels will become zero by applying some external torques to the spacecraft, when needed. It will be seen that this scheme will further reduce the occurrence of the singularity mentioned above.

The ideal purpose of the momentum management is to make the total angular momentum of the wheels zero or keep it within certain limits. Here it is assumed that zero total momentum is required, i.e., $\mathbf{A}\mathbf{h}_a = 0$, which implies that $\mathbf{h}_a \in N(\mathbf{A})$. For a cluster with identical wheels (the typical case), Eq. (5) implies $\boldsymbol{\omega}_c \in N(\mathbf{A})$. Recall now that singularity occurs when $\boldsymbol{\omega}_c \in R(\mathbf{A}^T)$. But $N(\mathbf{A}) = R(\mathbf{A}^T)^\perp$ and after momentum management the wheel angular velocity vector is orthogonal to the singularity subspace $R(\mathbf{A}^T)$. The possibility of singularity has thus been reduced as much as possible. This does not, of course, include the case when $\boldsymbol{\omega}_c = 0$, which belongs to both $N(\mathbf{A})$ and $R(\mathbf{A}^T)$. However, since for safety margin the energy stored in the wheels must always exceed the minimum energy level necessary for the spacecraft operation, the all-zero wheel angular velocity can only happen during initial satellite deployment when the wheels may be in a locked position. In this case, the wheel angular velocity initialization is performed after the deployment. In doing so, a torque in the null space of $\mathbf{A}$ is applied to the wheels to accelerate the wheel angular velocities to their normal operation range.

A simple momentum management scheme is adopted from Ref. 25. The torque required for momentum management is

$$\mathbf{g}_t = -k(\mathbf{A}\mathbf{h}_a - \mathbf{A}\mathbf{h}_{an}) \tag{33}$$

where $\mathbf{h}_{an}$ denotes the nominal angular momentum vector of the wheels, and $k > 0$ is a feedback control gain. For the purpose of momentum unloading and singularity avoidance here we choose $\mathbf{A}\mathbf{h}_{an} = 0$.

Numerical example

To demonstrate the aforementioned algorithm for the attitude and power tracking controller, the following numerical example has been performed. A near polar orbital satellite (orbital data chosen from the satellite Iridium 25578) is considered in this simulation.[19] The orbital elements are shown in Table 1. Here n is the orbital frequency, M_0 is

Table 1 Iridium 25578 orbital elements.

n (rev/day)	14.57788549
M_0 (deg)	234.7460
ω (deg)	125.5766
Ω (deg)	132.8782
i (deg)	86.5318
e	0.00216220
Epoch	05/23/1999 00:16:12.24

the mean anomaly at the epoch time, ω is the argument of perigee, Ω is the right ascension of the ascending node, i is the orbital inclination, and e is the eccentricity of the orbit. The satellite is assumed to have moment of inertia matrix in a principal axes system

$$\mathbf{I} = \begin{bmatrix} 200 & 0 & 0 \\ 0 & 200 & 0 \\ 0 & 0 & 175 \end{bmatrix} \text{ kg m}^2 \tag{34}$$

The four wheel cluster, shown in Fig. 1, is chosen for this simulation. The wheels are assumed to have the same axial moments of inertia. The $\mathbf{A}$ matrix in this case is given by

$$\mathbf{A} = \begin{bmatrix} 1 & 0 & 0 & \frac{\sqrt{3}}{3} \\ 0 & 1 & 0 & \frac{\sqrt{3}}{3} \\ 0 & 0 & 1 & \frac{\sqrt{3}}{3} \end{bmatrix} \tag{35}$$

The normal power requirement of this satellite is 680 Watts. However, it is required to be able to provide instantaneous peak power of 4 kW for up to 5 minutes. Considering the 34 minutes eclipse time and assuming that the 4 kW peak power lasts 5 minutes, the wheels should store at least 0.72 kWh energy. Taking into account a 100% safety margin, the wheels are required to store 1.5 kWh energy when they are fully charged. Suppose the nominal speed for the fourth wheel when the wheels are fully charged is -4000 rad/sec (-38,197 rpm), and the speed for the other three 2309.4 rad/sec (22,053 rpm). These speeds render zero total angular momentum of the wheels. The energy and the wheel speed require that each wheel has axial moment of inertia 0.338 kg m^2. Each energy/momentum wheel is assumed to provide a maximum torque 1 Nm.

The disturbance torque due to aerodynamics, solar pressure and other environmental factors is assumed to be[25]

$$\mathbf{g}_d = \begin{bmatrix} 4\times10^{-6} + 2\times10^{-6}\sin(nt) \\ 6\times10^{-6} + 3\times10^{-6}\sin(nt) \\ 3\times10^{-6} + 3\times10^{-6}\sin(nt) \end{bmatrix} \text{ N m} \tag{36}$$

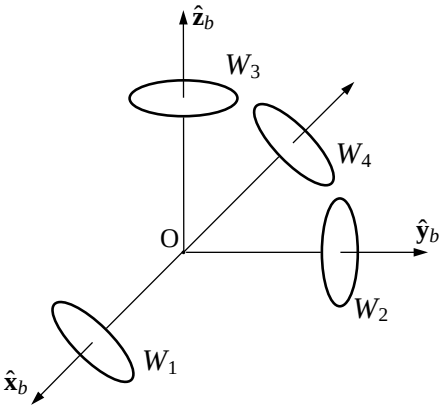

Fig. 1 The configuration of energy/momentum wheels.

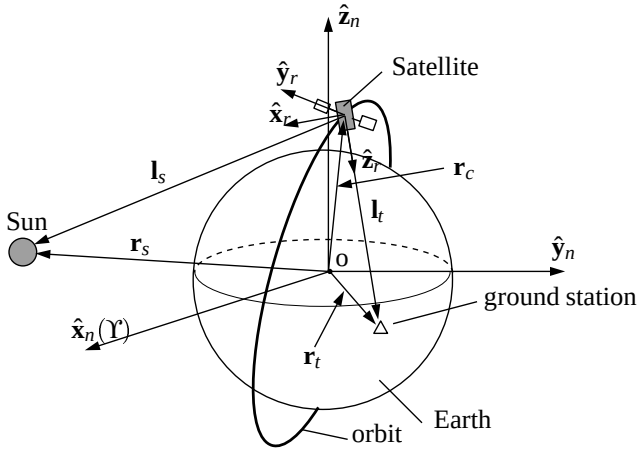

Fig. 2 The satellite mission illustration.

The satellite is required to perform Sun and ground station tracking as follows. The symmetry axis should point to a ground station while the satellite is rotated by this axis such that the solar panel is perpendicular to the vector from the satellite to the Sun. The ground station in this example is chosen to be Cape Canaveral (Longitude 80.467°W, Latitude 28.467°N). The Sun and the ground station are assumed to be always available to the satellite. In the following, we briefly describe the mission and the algorithm for obtaining the reference attitude maneuver history.

Mission definition

The scenario is shown in Fig. 2. The inertial frame is chosen to be the J2000 geocentric inertial coordinate system, denoted by the subscript n. The vectors $\mathbf{r}_s$, $\mathbf{r}_t$ and $\mathbf{r}_c$ denote the positions of the Sun, the ground station and the satellite, respectively, and the vector $\mathbf{l}_s$ and $\mathbf{l}_t$ denote the vectors from the satellite to the Sun and the ground station. The following coordinate systems are used in the simulation besides the inertial frame, shown in Figs. 3 and 4. Hereafter, $\hat{(\cdot)}$ denotes a unit vector, and $\dot{(\cdot)}$ denotes the derivative with respect to time, taken in the inertial frame.

- Local Vertical Local Horizontal (LVLH) orbital frame, $o\hat{\mathbf{x}}_l\hat{\mathbf{y}}_l\hat{\mathbf{z}}_l$, with the $\hat{\mathbf{z}}_l$ axis pointing towards the Earth center, the $\hat{\mathbf{y}}_l$ axis normal to the orbital plane and the $\hat{\mathbf{x}}_l$ axis completing the orthogonal frame.

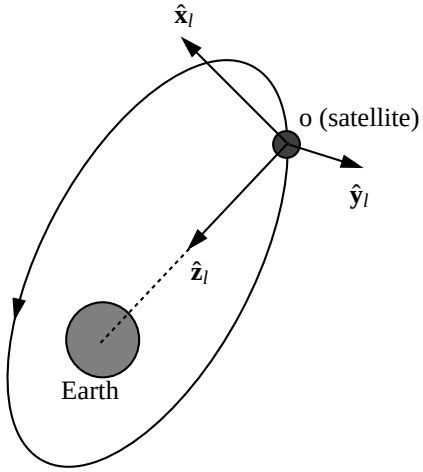

Fig. 3 The LVLH frame.

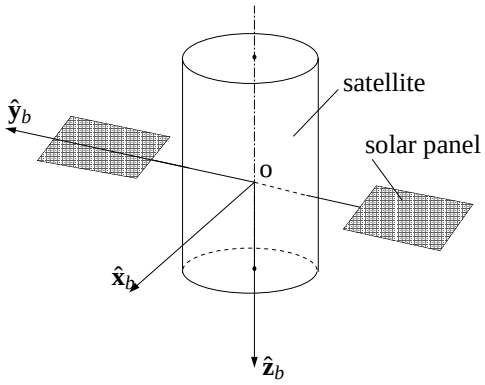

Fig. 4 The body frame of the satellite.

- Body frame, $o\hat{\mathbf{x}}_b\hat{\mathbf{y}}_b\hat{\mathbf{z}}_b$, with the $\hat{\mathbf{z}}_b$ axis along the boresight axis of the satellite, and the $\hat{\mathbf{y}}_b$ pointing along the solar panels.

The mission requires that at each moment along the orbit, the $\hat{\mathbf{z}}_b$ axis should track the ground station; i.e., $\hat{\mathbf{z}}_b$ tracks the unit vector along $\mathbf{l}_t$. In addition, the satellite should also track an attitude such that the $\hat{\mathbf{y}}_b$ axis is perpendicular to $\mathbf{l}_s$.

Computing the reference attitude profile

The satellite orbit is propagated by the orbit generator given in Ref. 26. From this, we know $\mathbf{r}_c$, $\dot{\mathbf{r}}_c$ and $\ddot{\mathbf{r}}_c$ in the inertial frame at any time. The Sun position ($\mathbf{r}_s$), velocity ($\dot{\mathbf{r}}_s$) and acceleration ($\ddot{\mathbf{r}}_s$) in the inertial frame are computed by the algorithm given in Ref. 27. The position ($\mathbf{r}_t$), velocity ($\dot{\mathbf{r}}_t$) and acceleration ($\ddot{\mathbf{r}}_t$) of the ground station in the inertial frame can be computed by converting the Universal Time (UT) into Greenwich Sidereal Time (GST).[26] From these, we know that

$$\mathbf{l}_s = \mathbf{r}_s - \mathbf{r}_c, \quad \dot{\mathbf{l}}_s = \dot{\mathbf{r}}_s - \dot{\mathbf{r}}_c, \quad \ddot{\mathbf{l}}_s = \ddot{\mathbf{r}}_s - \ddot{\mathbf{r}}_c \tag{37a}$$

$$\mathbf{l}_t = \mathbf{r}_t - \mathbf{r}_c, \quad \dot{\mathbf{l}}_t = \dot{\mathbf{r}}_t - \dot{\mathbf{r}}_c, \quad \ddot{\mathbf{l}}_t = \ddot{\mathbf{r}}_t - \ddot{\mathbf{r}}_c \tag{37b}$$

In the following, the attitude, angular velocity, and angular acceleration of the reference frame, which are the desired attitude, angular velocity, and angular acceleration for the body frame will be computed. The desired, or target, reference frame is denoted by $o\hat{\mathbf{x}}_r\hat{\mathbf{y}}_r\hat{\mathbf{z}}_r$ and is shown in Fig. 2.

The attitude reference

The rotation matrix $\mathbf{C}_N^L$ from the inertial frame to the LVLH frame can be readily computed by the orbital elements. Once the LVLH frame is known, we can write

$$\mathbf{l}_t = (\mathbf{l}_t \cdot \hat{\mathbf{x}}_l)\hat{\mathbf{x}}_l + (\mathbf{l}_t \cdot \hat{\mathbf{y}}_l)\hat{\mathbf{y}}_l + (\mathbf{l}_t \cdot \hat{\mathbf{z}}_l)\hat{\mathbf{z}}_l \tag{38}$$

so that

$$\hat{\mathbf{z}}_r = [(\mathbf{l}_t \cdot \hat{\mathbf{x}}_l)\hat{\mathbf{x}}_l + (\mathbf{l}_t \cdot \hat{\mathbf{y}}_l)\hat{\mathbf{y}}_l + (\mathbf{l}_t \cdot \hat{\mathbf{z}}_l)\hat{\mathbf{z}}_l]/\ell_t \tag{39}$$

where $\mathbf{l}_t = \ell_t \hat{\mathbf{l}}_t$. Since the $\hat{\mathbf{y}}_r$ axis is perpendicular to $\mathbf{l}_s$ and $\hat{\mathbf{z}}_r$, it can be computed by

$$\hat{\mathbf{y}}_r = \frac{\hat{\mathbf{z}}_r \times \hat{\mathbf{l}}_s}{|\hat{\mathbf{z}}_r \times \hat{\mathbf{l}}_s|} \tag{40}$$

and the $\hat{\mathbf{x}}_r$ axis is then given by

$$\hat{\mathbf{x}}_r = \hat{\mathbf{y}}_r \times \hat{\mathbf{z}}_r \tag{41}$$

From the unit vectors $\hat{\mathbf{x}}_r$, $\hat{\mathbf{y}}_r$, and $\hat{\mathbf{z}}_r$ we can compute $\mathbf{C}_N^R$, the rotation matrix from the inertial frame to the target reference frame. The value of $\eta_s = \hat{\mathbf{l}}_s \cdot \hat{\mathbf{y}}_b$ will be used as a condition for Sun tracking; i.e., $\eta_s = 0$ implies that the Sun is being tracked. In addition, the value $\eta_t = |\hat{\mathbf{l}}_t \times \hat{\mathbf{z}}_b|$ will be used as a condition for ground station tracking; i.e., $\eta_t = 0$ implies that the ground station is being tracked.

The angular velocity and the angular acceleration reference

We proceed to compute the angular velocity of the reference frame with respect to the inertial frame expressed in the target reference frame, $\boldsymbol{\omega}_R = [\omega_{rx},\ \omega_{ry},\ \omega_{rz}]^T$. The algorithm for computing ω_{rx} and ω_{ry} can be found in Ref. 28.

The derivative of the vector $\mathbf{l}_t$ in the inertial frame can be written in the desired reference frame as

$$\dot{\mathbf{l}}_t = (\dot{\mathbf{l}}_t \cdot \hat{\mathbf{x}}_r)\hat{\mathbf{x}}_r + (\dot{\mathbf{l}}_t \cdot \hat{\mathbf{y}}_r)\hat{\mathbf{y}}_r + (\dot{\mathbf{l}}_t \cdot \hat{\mathbf{z}}_r)\hat{\mathbf{z}}_r \tag{42}$$

Since $\dot{\mathbf{l}}_t$ can also be written as

$$\begin{aligned}\dot{\mathbf{l}}_t &= \frac{{}^R\mathrm{d}\mathbf{l}_t}{\mathrm{d}t} + \boldsymbol{\omega}_R \times \mathbf{l}_t \\ &= \frac{{}^R\mathrm{d}\mathbf{l}_t}{\mathrm{d}t} + \boldsymbol{\omega}_R \times (\ell_t \hat{\mathbf{z}}_r)\end{aligned} \tag{43}$$

where $\dfrac{{}^R\mathrm{d}\mathbf{l}_t}{\mathrm{d}t}$ is the derivative of $\mathbf{l}_t$ taken in the target reference frame. Comparison of Eq. (42) and Eq. (43) yields

$$\omega_{rx} = -\frac{\dot{\mathbf{l}}_t \cdot \hat{\mathbf{y}}_r}{\ell_t} \tag{44a}$$

$$\omega_{ry} = \frac{\dot{\mathbf{l}}_t \cdot \hat{\mathbf{x}}_r}{\ell_t} \tag{44b}$$

$$\frac{\mathrm{d}^R\mathbf{l}_t}{\mathrm{d}t} = \dot{\mathbf{l}}_t \cdot \hat{\mathbf{z}}_r \tag{44c}$$

Since $\hat{\mathbf{y}}_r \cdot \mathbf{l}_s = 0$, its time derivative is

$$\dot{\hat{\mathbf{y}}}_r \cdot \mathbf{l}_s + \hat{\mathbf{y}}_r \cdot \dot{\mathbf{l}}_s = 0 \tag{45}$$

Expanding the derivative terms in the above equation, we end up with

$$\omega_{rz} = \frac{\omega_{rx}\mathbf{l}_s \cdot \hat{\mathbf{z}}_r + \hat{\mathbf{y}}_r \cdot \dot{\mathbf{l}}_s}{\mathbf{l}_s \cdot \hat{\mathbf{x}}_r} \tag{46}$$

The angular acceleration vector $\dot{\boldsymbol{\omega}}_R = (\dot{\omega}_{rx},\ \dot{\omega}_{ry},\ \dot{\omega}_{rz})^T$ can be obtained by taking the derivatives of ω_{rx}, ω_{ry} and ω_{rz}. By doing so, we get

$$\dot{\omega}_{rx} = -\frac{\ddot{\mathbf{l}}_t \cdot \hat{\mathbf{y}}_r + 2\omega_{rx}\dot{\ell}_t}{\ell_t} + \omega_{ry}\omega_{rz} \tag{47a}$$

$$\dot{\omega}_{ry} = \frac{\ddot{\mathbf{l}}_t \cdot \hat{\mathbf{x}}_r - 2\omega_{ry}\dot{\ell}_t}{\ell_t} - \omega_{rx}\omega_{rz} \tag{47b}$$

$$\dot{\omega}_{rz} = \frac{\dot{M}N - M\dot{N}}{N^2} \tag{47c}$$

where

$$M = \omega_{rx}\mathbf{l}_s \cdot \hat{\mathbf{z}}_r + \hat{\mathbf{y}}_r \cdot \dot{\mathbf{l}}_s \tag{48}$$

$$N = \mathbf{l}_s \cdot \hat{\mathbf{x}}_r \tag{49}$$

$$\begin{aligned}\dot{M} = {} & \dot{\omega}_{rx}\mathbf{l}_s \cdot \hat{\mathbf{z}}_r + \omega_{rx}\dot{\mathbf{l}}_s \cdot \hat{\mathbf{z}}_r + \omega_{rx}\mathbf{l}_s \cdot (\boldsymbol{\omega}_R \times \hat{\mathbf{z}}_r) \\ & + \boldsymbol{\omega}_R \times \hat{\mathbf{y}}_r \cdot \dot{\mathbf{l}}_s + \hat{\mathbf{y}}_r \cdot \ddot{\mathbf{l}}_s\end{aligned} \tag{50}$$

$$\dot{N} = \dot{\mathbf{l}}_s \cdot \hat{\mathbf{x}}_r + \mathbf{l}_s \cdot (\boldsymbol{\omega}_R \times \hat{\mathbf{x}}_r) \tag{51}$$

Given $\boldsymbol{\omega}_R$ and $\dot{\boldsymbol{\omega}}_R$, the reference torque $\mathbf{g}_R$ is computed from Eq. (11).

Simulation results

With the reference satellite attitude profile computed in the previous section, we can apply the attitude and power tracking controller. Two simulations are conducted in sequence. First, a target acquisition maneuver is performed using the thrusters, where the satellite is maneuvered from the LVLH frame to the required Sun and ground station tracking attitude. Then the attitude control and energy storage functions are switched on and the energy/momentum wheels are used to keep tracking the Sun and the ground station. Here we assume that the wheels are spun up to their nominal angular velocities before deployment. This can be done using the power provided by the launch vehicle. If the

wheels are in the locked position (not spinning) after separation, a constant torque $\mathbf{g}_a = [1/\sqrt{3}\ \ 1/\sqrt{3}\ \ 1/\sqrt{3}\ \ -1]^T$ (Nm), which is in the null space of the matrix $\mathbf{A}$, can be used to spin the wheels up without disturbing the satellite motion. The power for this initial spin-up of the wheels can be provided by the solar panels of the satellite. A problem may occur in case the solar panels do not face the Sun at deployment. With body-mounted solar cells, it should not be a major concern, since some of the cells will be facing the Sun any time the spacecraft is in the sunlight. Another approach is to have a primary (non-rechargable) battery for the initial deployment/acquisition stage.

In the simulations, quaternions are used to describe the attitude from the inertial frame to the body and reference frames due to the large angle orbital maneuver, and MRPs are used to describe the difference between the body and the reference frame. The results are presented in the following two subsections.

Target acquisition

Before the satellite can be operated to track the Sun and the ground station, target acquisition has to be performed so that the satellite is maneuvered to obtain the right attitude in order to start continuous tracking. The simulation starts with the satellite body frame aligned with the LVLH frame. Because this initial target acquisition maneuver is usually a fast, large angle (slew) maneuver and the wheels are of fairly low control authority (1 Nm in this example), external thrusters have to be used to issue the required torque; i.e., in Eq. (17), we choose

$$\mathbf{A}\mathbf{g}_a = 0 \tag{52}$$

$$\begin{aligned}\mathbf{g}_t = &-\mathbf{h}_B^{\times}\mathbf{J}^{-1}(\mathbf{h}_B - \mathbf{A}\mathbf{h}_a) - \mathbf{g}_g + \mathbf{J}\boldsymbol{\omega}_B^{\times}\delta\boldsymbol{\omega} \\ &+ \mathbf{J}\mathbf{C}_R^B(\delta\boldsymbol{\sigma})\mathbf{J}^{-1}\mathbf{h}_R^{\times}\mathbf{J}^{-1}\mathbf{h}_R + \mathbf{J}\mathbf{C}_R^B(\delta\boldsymbol{\sigma})\mathbf{J}^{-1}\mathbf{g}_R \\ &- k_1\delta\boldsymbol{\omega} - k_2\delta\boldsymbol{\sigma}\end{aligned} \tag{53}$$

The controller gains are chosen as $k_1 = 24$ and $k_2 = 27$. Figure 5 shows the angular velocity tracking error of the satellite, and Fig. 6 shows the quaternions of the body frame and the reference frame. It is seen that after about 70 sec the satellite attitude tracks the reference. In Fig. 7 it is shown that the Sun tracking condition value η_s goes to zero after about 90 seconds. In Fig. 8 it is shown that the ground station tracking condition value η_t goes to zero also after about 90 seconds. Figure 9 shows the torque required to perform the target acquisition maneuver.

Continuous tracking

After the satellite tracks the Sun and the ground station, the energy/momentum wheel attitude and power tracking control is switched on, so that the satellite will keep tracking the Sun and the ground station. In this case, the wheels will provide both the target tracking torques and the energy storage torques. The thrusters will only be used to issue the

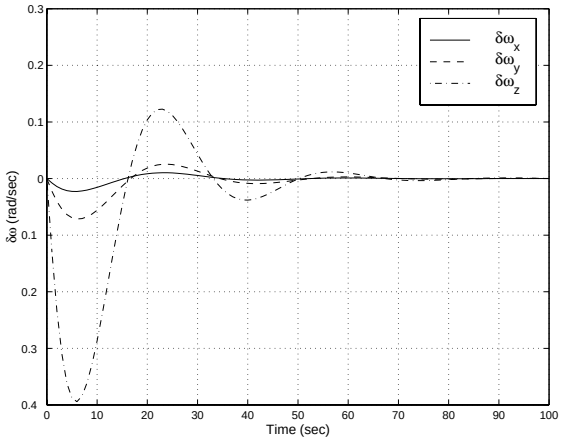

Fig. 5 The error in angular velocity of the satellite during target acquisition.

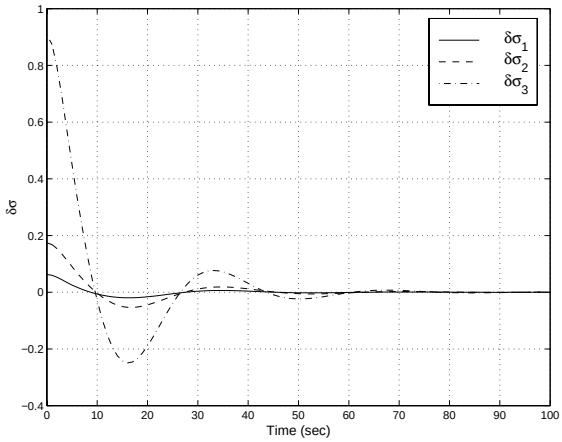

Fig. 6 Attitude error during target acquisition.

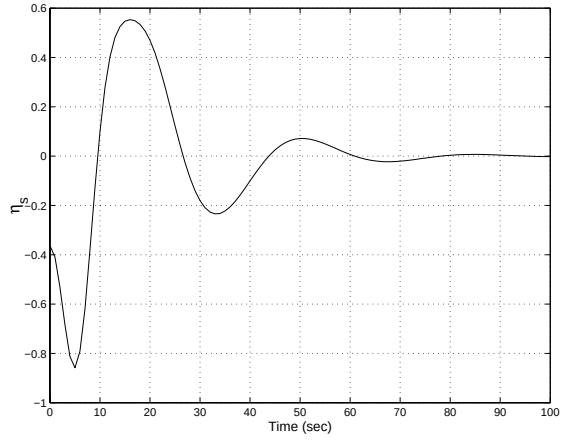

Fig. 7 The Sun tracking condition during target acquisition ($\eta_s = \hat{\mathbf{l}}_s \cdot \hat{\mathbf{y}}_b$).

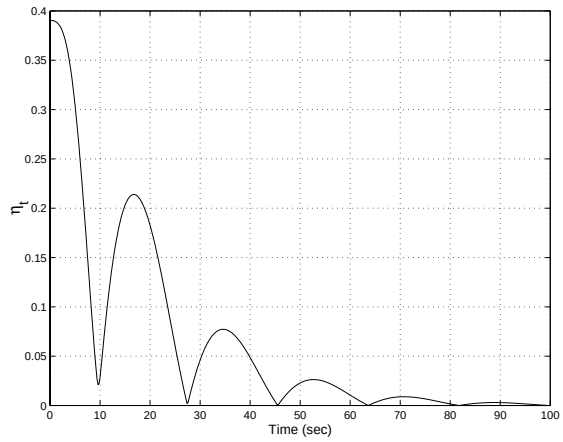

Fig. 8 The ground station tracking condition during target acquisition ($\eta_t = |\hat{\mathbf{l}}_t \times \hat{\mathbf{z}}_b|$).

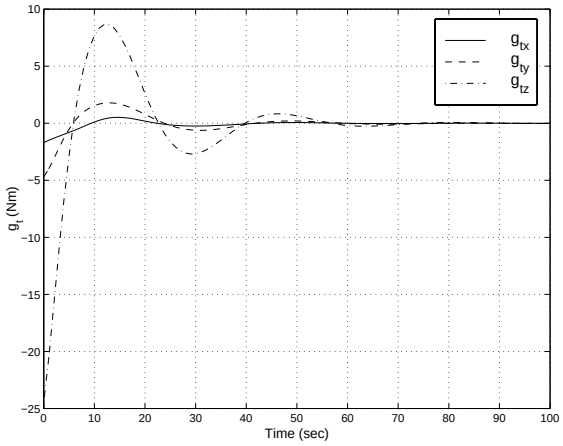

Fig. 9 The required thruster torque for the target acquisition ($\mathbf{g}_a = 0$).

necessary momentum management torque; i.e., in Eq. (17), we choose

$$\mathbf{g}_t = -k(\mathbf{Ah}_a - \mathbf{Ah}_{an}) \quad \text{every two orbits} \tag{54}$$

and

$$\begin{aligned}\mathbf{Ag}_a =& \mathbf{h}_B^{\times}\mathbf{J}^{-1}(\mathbf{h}_B - \mathbf{Ah}_a) + \mathbf{g}_t + \mathbf{g}_g - \mathbf{J}\boldsymbol{\omega}_B^{\times}\delta\boldsymbol{\omega} \\ & - \mathbf{J}\mathbf{C}_R^B(\delta\boldsymbol{\sigma})\mathbf{J}^{-1}\mathbf{h}_R^{\times}\mathbf{J}^{-1}\mathbf{h}_R - \mathbf{J}\mathbf{C}_R^B(\delta\boldsymbol{\sigma})\mathbf{J}^{-1}\mathbf{g}_R \\ & + k_1\delta\boldsymbol{\omega} + k_2\delta\boldsymbol{\sigma}\end{aligned} \tag{55}$$

The simulation orbit starts from 02/23/99 07:59:32.28 and lasts for 25,000 seconds (about 4 orbits). The controller gains are chosen as $k_1 = 24$, $k_2 = 27$, and $k = 0.005$. During the eclipse, the nominal power requirement during eclipse is 680 W, with an additional requirement of 4 kW power for 5 minutes. During sunlight, the wheels are charged with a power level of 1 kW until the total energy stored in the wheels reaches 1.5 kWh. After the wheels are charged, the momentum management is switched on every two orbits. Figures 10 and 11 show the angular velocity and attitude error during tracking. The angular velocity errors are practically zero for the whole period of the maneuver. The largest errors occur at the times of the highest wheel momenta; compare with Fig. 15. The attitude error in Fig. 11

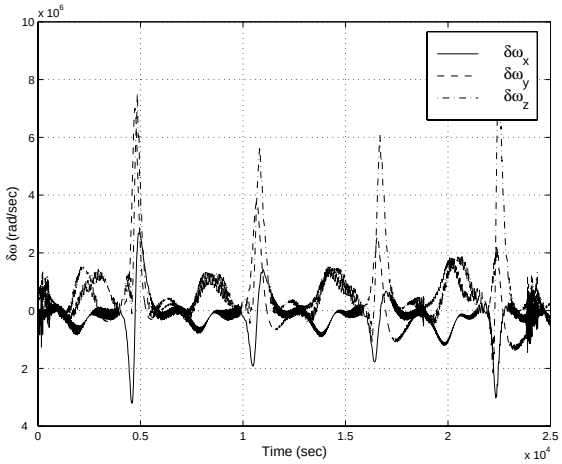

Fig. 10 Angular velocity error during tracking.

corresponds to a pointing error of less than 0.1 deg about all three axes. Figures 12 and 13 show that the Sun and ground station tracking conditions are being satisfied. Figure 14 shows the power profile with the sunlight and eclipse indication, where sunlight is indicated by 1 and eclipse is indicated by -1. The corresponding torque applied by the wheels is shown in Fig. 15, along with the total angular momentum of the wheels. As expected, the wheels charge during sunlight and discharge during the eclipse. Every two orbits (at about 0.6×10^4 and 1.8×10^4 seconds in Fig. 15) the total angular momentum of the wheels, $\mathbf{Ah}_a$ goes to zero due to proper momentum management. Finally, Fig. 16 shows the wheel speeds.

These plots indicate that there are no major theoretical problems in using a cluster of four or more energy/momentum wheels in a suitable geometric configuration to successfully control the attitude and power requirements of a satellite in a typical Earth orbit scenario. In reality, several issues need to be addressed prior to the implementation of such a control law for an IPACS. For instance, vibration suppression algorithms for high-speed flywheels, proper rotor sizing and containment issues are of great interest in that respect. These and other similar issues are left for future investigation.

Conclusions

In this paper, we develop an algorithm for controlling the spacecraft attitude while simultaneously tracking a desired power profile, using a cluster of more than three noncoplanar energy/momentum wheels. The torque is decomposed into two perpendicular spaces. One is the null space of this matrix whose columns are the unit vectors along the axes of each wheel. The torque in this space is used to track the required power level of the wheels, while the torque in the space perpendicular to the null space of this matrix is used to control the attitude of the satellite. The torque decomposition is based on solving a set of linear equations. Singularities may occur in case the coefficient matrix does

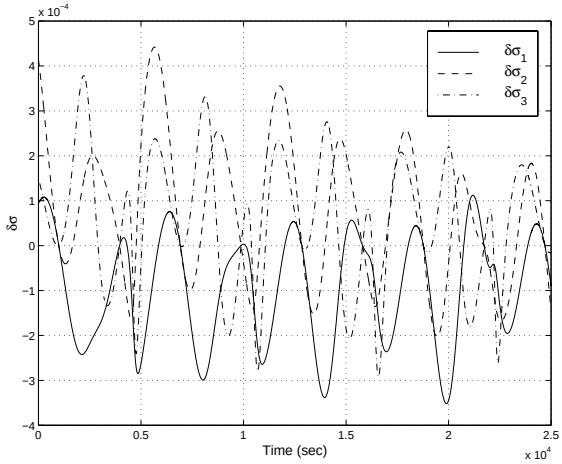

Fig. 11 Attitude error during tracking.

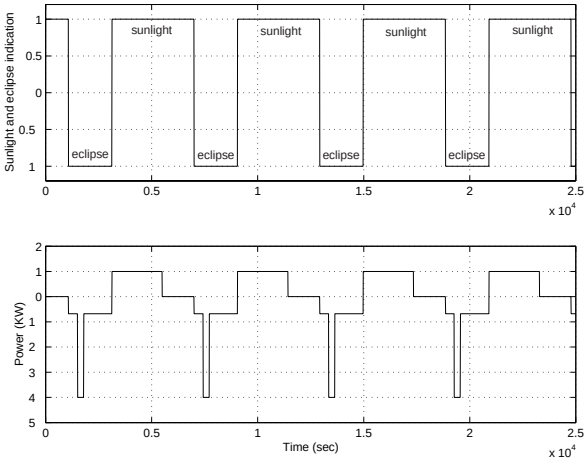

Fig. 14 Sunlight/eclipse indication and power profile.

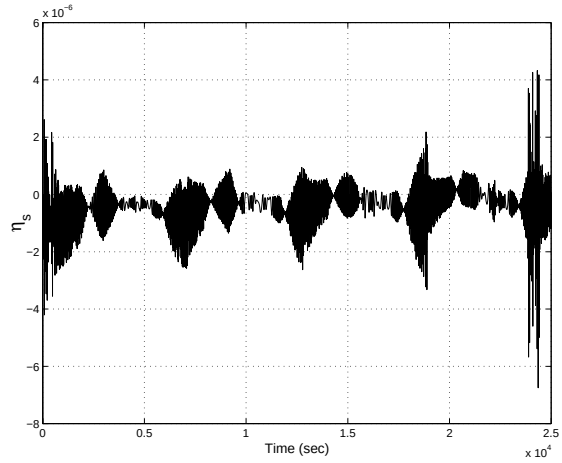

Fig. 12 The Sun tracking condition during tracking ($\eta_s = \mathbf{l}_s \cdot \hat{\mathbf{y}}_b$).

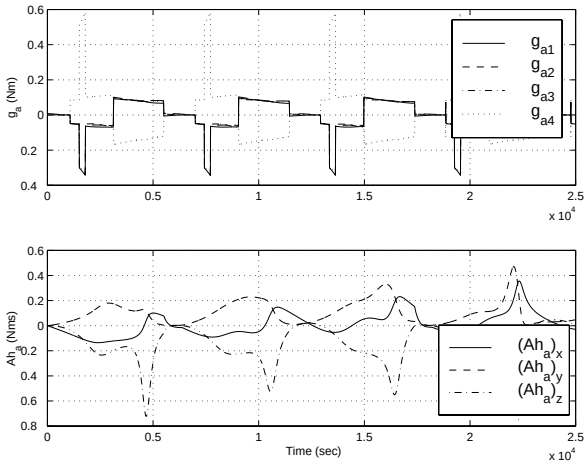

Fig. 15 The axial torques and the total angular momentum of the energy/momentum wheels.

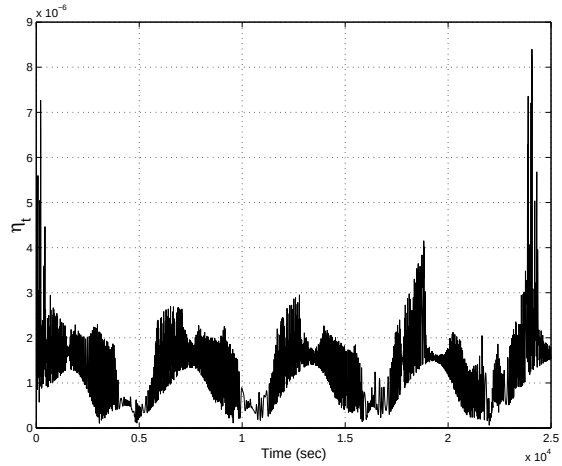

Fig. 13 The ground station tracking condition during tracking ($\eta_t = |\mathbf{l}_t \times \hat{\mathbf{z}}_b|$).

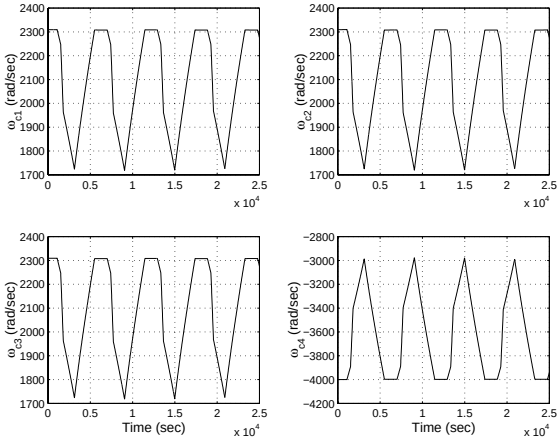

Fig. 16 The angular velocities of the energy/momentum wheels .

not have full row rank. In this case, no arbitrary power profile can be tracked. A momentum management scheme is considered to null the total angular momentum of the wheels in order to minimize the gyroscopic effects and also prevent the occurrence of singularities. A numerical example based on a realistic scenario for an Iridium-type satellite demonstrates the efficacy of the proposed algorithm.

References

[1]Wertz, J. and Larson, W., editors, *Space Mission Analysis and Design*, Kluwer Academic Publishers, Boston, 1991, pp. 349–369.

[2]Roes, J. B., "An Electro-Mechanical Energy Storage System for Space Application," *Progress in Astronautics and Rocketry*, Vol. 3, Academic Press, New York, 1961, pp. 613–622.

[3]Anderson, W. W. and Keckler, C. R., "An Integrated Power/Attitude Control System (IPACS) for Space Application," *Proceedings of the 5th IFAC Symposium on Automatic Control in Space*, 1973.

[4]Cormack III, A., "Three Axis Flywheel Energy and Control Sytems," NASA Technical Report TN-73-G&C-8, North American Rockwell Corp., 1973.

[5]Keckler, C. R. and Jacobs, K. L., "A Spacecraft Integrated Power/Attitude Control System," *9th Intersociety Energy Conversion Engineering Conference*, 1974, pp. 20–25.

[6]Will, R. W., Keckler, C. R., and Jacobs, K. L., "Description and Simulation of an Integrated Power and Attitude Control System Concept for Space-Vehicle Application," NASA Technical Report TN D-7459, NASA, 1974.

[7]Notti, J. E., Cormack III, A., Schmill, W. C., and Klein, W. J., "Integrated Power/Attitude Control System (IPACS) Study: Volume II–Conceptual Designs," NASA Technical Report CR-2384, Rockwell International Space Division, Downey, CA, 1974.

[8]Rodriguez, G. E., Studer, P. A., and Baer, D. A., "Assessment of Flywheel Energy Storage for Spacecraft Power Systems," NASA Technical Memorantum TM-85061, NASA Goddard Space Flight Center, Greenbelt, MD, 1983.

[9]Gross, S., "Study of Flwheel Energy Storage for Space Stations," NASA Technical Report CR-171780, Boeing Aerospace Co., Seattle, WA, 1984.

[10]Anand, D., Kirk, J. A., and Frommer, D. A., "Design Considerations for Magnetically Suspended Flywheel systems," *Proceedings of the 20th Intersociety Energy Conversion Engineering Conference*, Vol. 2, 1985, pp. 449–453.

[11]Anand, D., Kirk, J. A., Amood, R. B., Studer, P. A., and Rodriguez, G. E., "System Considerations for Magnetically Suspended Flywheel systems," *Proceedings of the 21st Intersociety Energy Conversion Engineering Conference*, Vol. 3, 1986, pp. 1829–1833.

[12]Downer, J., Eisenhaure, D., Hockney, R., Johnson, B., and O'Dea, S., "Magnetic Suspension Design Options for Satellite Attitude Control and Energy Storage," *Proceedings of the 20th Intersociety Energy Conversion Engineering Conference*, Vol. 2, 1985, pp. 424–430.

[13]Flatley, T., "Tetrahedron Array of Reaction Wheels for Attitude Control and Energy Storage," *Proceedings of the 20th Intersociety Energy Conversion Engineering Conference*, Vol. 2, 1985, pp. 2353–2360.

[14]O'Dea, S., Burdick, P., Downer, J., Eisenhaure, D., and Larkin, L., "Design and Development of a High Efficiency Effector for the Control of Attitude and Power in Space Systems," *Proceedings of the 20th Intersociety Energy Conversion Engineering Conference*, Vol. 2, 1985, pp. 353–360.

[15]Oglevie, R. E. and Eisenhaure, D. B., "Advanced Integrated Power and Attitude Control System (IPACS) Technology," NASA Technical Report CR-3912, NASA, November, 1985.

[16]Oglevie, R. E. and Eisenhaure, D. B., "Integated Power and Attitude Control System (IPACS) Technology," *Proceedings of the 21st Intersociety Energy Conversion Engineering Conference*, Vol. 3, 1986, pp. 1834–1837.

[17]Olmsted, D. R., "Feasibility of Flywheel Energy Storage in Spacecraft Applications," *Proceedings of the 20th Intersociety Energy Conversion Engineering Conference*, Vol. 2, 1985, pp. 444–448.

[18]Studer, P. and Rodriguez, E., "High Speed Reaction Wheels for Satellite Attitude Control and Energy Storage," *Proceedings of the 20th Intersociety Energy Conversion Engineering Conference*, Vol. 2, 1985, pp. 349–352.

[19]Fossa, C. E., Raines, R. A., Gunsch, G. H., and Temple, M. A., "An Overview of the IRIDIUM Low Earth Orbit (LEO) Satellite System," *Proceedings of the IEEE National Aerospace and Electronics Conference*, (Dayton, OH), Institute of Electrical and Electronics Engineers, Inc., Piscataway, NJ, 1998, pp. 152–159.

[20]Hughes, P., *Spacecraft Attitude Dynamics*, John Wiley & Sons, New York, 1986, pp. 233–248.

[21]Tsiotras, P., "Stabilization and Optimality Results for the Attitude Control Problem," *Journal of Guidance, Control, and Dynamics*, Vol. 19, No. 4, 1996, pp. 772–777.

[22]Shuster, M. D., "A Survey of Attitude Representations," *Journal of the Astronautical Sciences*, Vol. 41, No. 4, 1993, pp. 439–517.

[23]Hall, C., Tsiotras, P., and Shen, H., "Tracking Rigid Body Motion Using Thrusters and Reaction Wheels," *Astrodynamics Specialists Conference*, Boston, MA., August 10-12 1998, AIAA Paper 98-4471.

[24]Hall, C., "High-Speed Flywheels for Integrated Energy Storage and Attitude Control," *American Control Conference*, Vol. 3, 1997, pp. 1894–1898.

[25]Sidi, M., *Spacecraft Dynamics and Control, A Practical Engineering Approach*, Cambridge University Press, New York, 1997, pp. 241–242.

[26]Wertz, J., editor, *Spacecraft Attitude Determination and Control*, Reidel, Boston, 1997, pp. 132–138.

[27]Meeus, J., *Astronomical Algorithms*, Willmann-Bell, Richmond, Virginia, 1991, Chaps. 21,24,25,31 and Appendices.

[28]Hablani, H., "Design of a Payload Pointing Control system for Tracking Moving Objects," *Journal of Guidance, Control, and Dynamics*, Vol. 12, No. 3, 1989, pp. 365–374.